Interface Affected Polymer Dynamics: NMR, SANS, and DLS Study of the Influence of Shell−Core Interactions on the Core Chain Mobility of Poly(2-ethylhexyl acrylate)-*block*-poly(acrylic acid) Micelles in Water

J. Kříž,* J. Pleštil, Z. Tuzar, H. Pospíšil, J. Brus, J. Jakeš, B. Masař, P. Vlček, and D. Doskočilová

Institute of Macromolecular Chemistry, Academy of Sciences of the Czech Republic, Heyrovsky Sq. 2, 16206 Prague 6, Czech Republic

Received June 15, 1998

ABSTRACT: Mobility of side chain groups in the essentially fluid core of acrylate−acrylic acid block copolymer micelles has been examined by a multiquantum NMR relaxation study supported by ^{1}H high resolution and MAS spectra and a SANS and DLS study of the physical structure of the micellar systems. It is shown that poly(2-ethylhexyl acrylate)-*block*-poly(acrylic acid) (**PEHA−PAA)** and its sodium salts of a composition $\mathbf{EHA_{53}AA_{279}}$ form micelles in water or D_2O with a **PEHA** core radius of about 4.7 nm, containing about 40 copolymer molecules according to SANS. The apparent core radius increases with lower neutralization degree of the **PAA** units reaching 6.7 nm in the purely acidic form. This difference is shown by NMR to be due to an increasing layer of a mixed interface containing units of both **PEHA** and **PAA**. The overall radius of the micelle in the form neutralized at least to 10 mol % has been estimated to be 24 nm by SANS, the hydrodynamic radius obtained by DLS in a fully neutralized form was 28 nm, and the rotational hydrodynamic radius estimated from ^{1}H MAS and static NMR was 26−27 nm. The mostly acidic form of **PEHA−PAA** tends to form aggregates which can be dispersed by ultrasound. Using NMR spectra with various degrees of T_2-filtration, dipolar interaction canceling by pulse sequence, MAS under various spinning rates, and signal shape analysis under varied viscosity of the medium and mobility of the shell blocks, a varying restriction or hindrances of segmental motion both in the inner part of the shell and in the micellar core can be demonstrated. Using transverse and rotating frame relaxation in varying regime and processing of data, approximate spectra of the transverse relaxation times for the side-group methyl and methylene signals can be reconstructed. According to them, about a third of the side groups possess a mobility comparable to that in bulk **PEHA** whereas the remaining part is perceptibly hindered in motion, in particular that near to the core−shell interface. Monomer **EHA** was swollen into the core and polymerized by γ-irradiation offering thus 0.78−0.57 free **PEHA**/bound core **PEHA**. Although this dilution of the core blocks led to some increase in mobility, no chains or their side groups acquired mobility equivalent to that in bulk **PEHA** at the same temperature. The results are discussed in terms of resistance against motional core−shell group exchange and osmotic pressure on the core−shell interface.

Introduction

The spontaneous self-assembly of amphiphilic block copolymers into fairly uniform polymer micelles[1−7] can be grossly explained by the interplay of hydrophilic and hydrophobic interactions of their blocks with the medium, i.e., by the net gain in negative free energy caused by the negative enthalpy surpassing the simultaneous entropy loss. Such a model neglects, however, some subtler effects which could prove to be of utmost importance when higher degrees of self-organization will be reached. One of them is the effect of the interface itself, in our case the core−shell interface, on the mobility and penetrability of the polymer segments forming the micellar core. In our previous studies[8−10] utilizing the complementary advantages of NMR and scattering methods we have already found some influence of the ionization state of the poly(acrylic acid) (**PAA**) shell of the micelle on the penetrability and swelling capacity of its core. In a recent study,[11] we have noticed that the chain mobility of the poly(2-ethylhexyl acrylate) (**PEHA**) blocks in the inner core of three-layer micelles of poly(2-ethylhexyl acrylate)-*block*-poly(methyl methacrylate)-*block*-poly(acrylic acid) copolymers is grossly diminished in comparison to that in bulk **PEHA**. In that case, this behavior could be explained by the arrested motion of the **PEHA** part linked to the quasi-glassy poly(methyl methacrylate) (**PMMA**) layer. Comparative results with the simpler poly(2-ethylhexyl)-acrylate-*block*-poly(acrylic acid) (**PEHA−PAA**) indicated, however, that even in the absence of the **PMMA** layer there is a difference in **PEHA** mobility between the micellized **PEHA−PAA** copolymer and bulk **PEHA** homopolymer. We devote this separate study to this problem.

Experimental Section

Block copolymers and micellar solutions. Poly(2-ethylhexyl acrylate)-*block*-poly(acrylic acid) (**PEHA−PAA**) copolymer was prepared[12] by a sequential anionic polymerization of *tert*-butyl acrylate (**tBuA**) and 2-ethylhexyl acrylate (**EHA**) in a toluene−THF 9:1 vol/vol mixture using initiation by a methyl 2-lithioisobutyrate−lithium *tert*-butoxide (1:4) system at 195 K and subsequent selective acidolysis of the poly(**tBuA**) block using the method described earlier.[8] The molecular weights and polydispersities of the poly(**tBuA**) prepolymer and the resulting poly(**tBuA**)-*block*-poly(**EHA**) were established by SEC using THF and the constants[13] $K = 3.3 \times 10^{-5}$ and $a = 0.80$ for both polymers. The **PtBuA** prepolymer had the average values $M_n = 35\,804$, $M_w = 36\,480$ and $M_z = 37\,163$ according to SEC; i.e., polydispersity $M_w/M_n = 1.02$. The resulting **PtBuA−PEHA** block copolymer had $M_n = 45\,614$, $M_w = 45\,660$ and $M_z = 47\,491$; i.e., again polydispersity $M_w/M_n = 1.02$. The M_n increase after the second polymerization step exactly corresponds to **EHA** conversion; i.e., all the **PtBuA** chains were living and formed a block copolymer. SEC chromatograms of the prepolymer and final product show that all

10.1021/ma9809334 CCC: $18.00 © 1999 American Chemical Society
Published on Web 01/05/1999

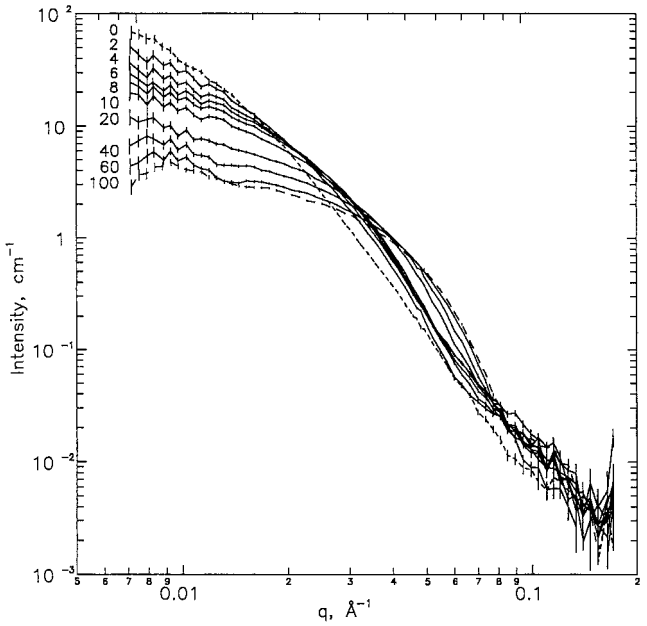

Figure 1. Experimental SANS curves for the **PEHA**−**PAA** particles in D_2O.The numbers on the curves denote the degree of neutralization with NaOH in percent.

PtBuA chains took part in the copolymerization and no poly(**EHA**) homopolymer was formed. ^1H and ^{13}C NMR spectra of the product are exact superpositions of the corresponding spectra of **PtBuA** and **PEHA** and differ from those of a **EHA**−**tBuA** statistical copolymer. In other words, no trace of statistical copolymerization can be observed. Taking the coincidence of M_n increase and conversion in the second step, the very low polydispersity after the first and second steps, the shape of the corresponding SEC chromatograms, and NMR spectra, we can conclude that the product is a pure block copolymer. NMR analysis established the molar ratio of **EHA/tBuA** in the product to be about 53/279 (calculated for an average molecule) as expected from the ratio of the reaction components and their conversion. After selective hydrolysis of the block copolymer, the **PEHA**−**PAA** product was again analyzed by NMR in THF-d_8−D_2O 2:1 v/v at 330 K. The hydrolysis was found to be completed up to 99.6% and the relation of the two comonomers unchanged.

To prepare its micellar form, the selectively hydrolyzed **PEHA**−**PAA** product was dissolved in a THF−water (2:1 w/w) mixture, transferred into distilled water by dialysis and freeze-dried.[8] For NMR and SANS experiments, the freeze-dried product was directly dissolved either in D_2O or in the solution of the appropriate amount of NaOH in D_2O. For DLS experiments, the product was redissolved in THF−water mixture and transferred to distilled water by dialysis.

NMR Measurements. 300.13 MHz ^1H NMR spectra of mostly 0.5% w/w solutions of the block copolymers in D_2O (99.8% d) were measured with a Bruker Avance DPX 300 spectrometer using 0.01% by weight of sodium 2,2-dimethyl-2-silapentane-5-sulfonate (DSS) as external standard. As a rule, 80 scans with selective presaturation of the remaining H_2O were done and the exponential weighting (line broadening 2 Hz) was used before Fourier transform. T_1 and T_2 were measured using conventional inversion−recovery and Carr−Purcell−Meiboom−Gill (CPMG) sequence with the delay between the π pulses equal to 0.8−2 ms. To check the effect of J-modulation on the spin−echo in T_2 experiments, saturation modulated spin−echo experiments were done in which the signal coupled to the measured one was saturated by selective irradiation during the pulse sequence. 2D measurements of T_2 distributions were measured using incremented phase of both the pulses and receiver (TPPI scheme) and phase sensitive Fourier transform in both dimensions. T_2-filtered spectra were measured with the sequence $d_1-\pi/2_x-[\tau-\pi_y-2\tau-\pi_{-y}-\tau]_n-$FID, the phases being circled according to the usual CYCLOPS scheme. With the length of the π pulse expressed in seconds, the filtering delay d_f has the value $d_f = n(2\pi + 4\tau)$.

In evaluation of relaxation experiments, both peak and integral (area) intensities were used. When spectra were compared under various regimes, i.e., swelling degree or spinning rate, absolute integral intensities of deconvoluted signals were used.

^1H NMR static, MAS, and Hahn−echo MAS spectra were measured at 200 MHz with a Bruker Avance DSX 200 spectrometer at 298 and 320 K using spinning rates of 2, 4, 8, and 15 kHz. A high-resolution ZrO_2 rotor with a HR spacer and KEL-F caps was used for MAS of liquid samples.

Small-Angle Neutron Scattering (SANS) Measurements. SANS measurements were performed using the time-of-flight small-angle neutron spectrometer YuMO at the IBR-2 pulse reactor in the Joint Institute for Nuclear Research, Dubna,[14] Czech Republic. The solution was placed in an optical quartz cell with a path length of 2 mm. All measurements were corrected for background scattering and normalized using a vanadium standard.[15] Scattering data are presented as a function of the magnitude of the scattering vector, $q = (4\pi/\lambda) \sin\theta$, where λ is the wavelength and 2θ is the scattering angle.

Parameters of the micellar cores were obtained by fitting of scattering curve for homogeneous spherical particles with a two-parameter Schulz−Zimm distribution of radii to the SANS data. Adjustable parameters of the distribution were the mean radius, R_m, and the width parameter, Z, related to the relative standard deviation as $\sigma/R_m = \sqrt{1/(Z+1)}$.

The initial part of each SANS curve, which is usually affected by the scattering from the micelle shell and by the interparticle interference, was not taken into account. The formulas used in the fitting were given previously.[11]

Determination of the parameters describing the particles as a whole (radius of gyration, R_g, molar mass) was based on the Guinier analysis of the SANS curves.

Dynamic Light Scattering (DLS). The measurements of hydrodynamic radii, R_H, were made[16] using an multibit, multi-tau ALV 5000 autocorrelator with an argon ion laser (λ_0 = 514.5 nm). Data were processed using a standard cumulant method.

Results and Discussion

The dynamics of the micellar system reflected in its NMR spectral behavior consists of local motions of individual groups, segmental motions of the polymer chains or their respective blocks in the micellar core and shell, and the collective tumbling of the whole micelles or their aggregates. As these motions, in particular the last ones, depend on the geometry and structure of the system, we start our analysis with the results of neutron and light scattering. We then analyze the influence of the physical structure and behavior of the micellar system on its NMR spectra, and after having separated its various factors, we proceed to the analysis of the local mobility of the observable groups in the micellar core using NMR relaxation. To discern the effect of the chain end being attached to the core−shell interface and that of the mere confinement of the chain in the restricted space of the core, we then repeat the same analysis on micelles with cores swollen with **PEHA** homopolymer.

Characterization of the Micelles and Their Aggregates by Neutron and Light Scattering. Figure 1 shows the SANS curves of the poly(2-ethylhexyl acrylate)-*block*-poly(acrylic acid) (**PEHA**−**PAA**) solutions at various degrees of neutralization (α) of the **PAA** shell with NaOH. The decrease in the scattering intensity at the smallest angles with increasing α indicates that neutralization of **PAA** leads to formation of smaller particles.

Table 1. SANS Characteristics of the PEHAPAA Particles at Various Degree of Neutralization

α	R_{core}, nm	σ/R_{core}	V_{core}, 10^3 nm^3	micellar molar mass, 10^6g/mol		R_g, nm	R_{mic}, nm
0[a]						8.3	14.1	
0						10.2	15.1	
0.02						7.0	13.5	
0.04						5.0	12.2	
0.06	6.7	0.33	3.6	7.5	7.3	3.8	11.0	21
0.08	6.7	0.30	3.1	6.7	6.4	3.3	10.7	20
0.10	6.5	0.28	2.5	5.5	4.9	2.6	10.1	19
0.20	5.6	0.26	1.5	3.3	3.0	1.4	8.7	16
0.40	5.1	0.24	1.1	2.3	2.1	1.1	9.0	17
0.60	4.9	0.21	0.79	1.7	1.5	1.1	11.3	23
1.00	4.7	0.22	0.73	1.6	1.3	1.1	10.2	22

[a] Ultrasonic treatment.

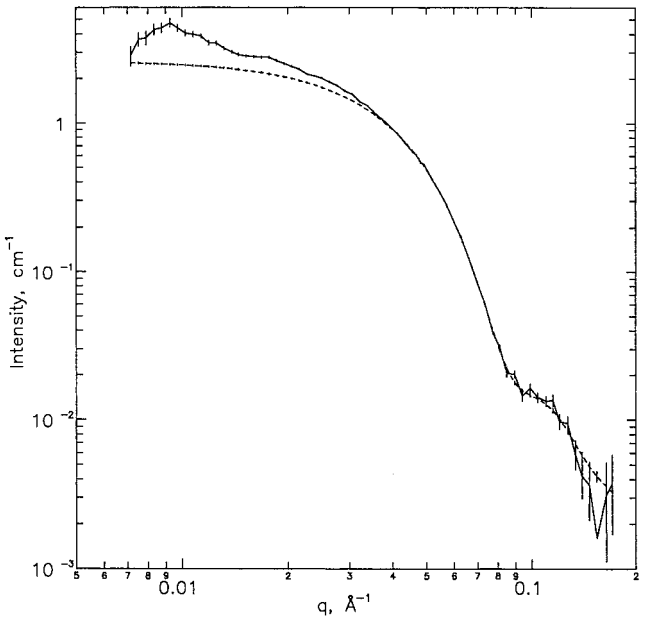

Figure 2. Least-squares fit of the scattering function of polydisperse spherical particles (dashed line) to experimental SANS curve (solid line) of the **PEHA−PAANa** micelles. The fit provided the mean radius of the micelle core (R_{core} = 4.7 nm) and relative standard deviation (σ/R_{core} = 0.22).

The size and mass of the particles was assessed using the Guinier approximation of the SANS curves. This approximation provides the radius of gyration, R_g, and intensity extrapolated to zero scattering angle, $I(0)$. From the latter quantity, we calculated molar mass of the particles as[17]

$$M_w^{Guin} = \frac{I(0)N_A}{c(\Delta b)^2} \tag{1}$$

where c is the copolymer concentration, N_A is the Avogadro constant, $\Delta b = b - \rho_0$ is the excess scattering amplitude, b is the scattering amplitude and partial specific volume of the copolymer, and ρ_0 is the scattering density of the solvent.

An alternative way of determining the size and mass of the particles was based on the assumption that the particles have architecture typical of micelles. We assume that the insoluble **PEHA** blocks form a core, which is surrounded by swollen **PAA** chains. The core characteristics were determined by a least-squares fit of the scattering function for spherical particles to the SANS curves in a higher-q region where the data are presumably not strongly affected by the scattering contribution of the micelle shell.

The fit provides the mean radius, R_{core}, polydispersity, σ/R_{core}, and the mean volume, V_{core}, of the core (Table 1). Figure 2 shows an example of the fit. The micelle mass can be expressed in terms of the core volume, V_{core}, and density, d_{core}, as

$$M_w^V = V_{core} d_{core} N_A / w_{core} \tag{2}$$

where w_{core} is the weight fraction of the core-forming blocks in the copolymer.

The micelle mass was also calculated from the extrapolated intensity, $I_{core}(0)$, using a formula similar to eq 1.

$$M_w^I = \frac{I_{core}(0)N_A}{c(\Delta b)_{core}^2 w_{core}^2} \tag{3}$$

Contrary to a calculation based on eq 2, which relies on the shape of the SANS curves, this approach requires the absolute intensities, copolymer concentration and the contrast factor of the core-forming polymer.

A rough estimate of the overall radius of the micelles, R_{mic}, was obtained from the radius of gyration, R_g, using the formula valid for two-component spherical particles

$$R_g^2 = f_1 R_{g,1}^2 + (1 - f_1) R_{g,2}^2 \tag{4}$$

where f_1 is the relative excess scattering amplitude of component 1, and $R_{g,1}$ and $R_{g,2}$ are the radii of gyration of the single components. Within the core/shell model the radii of gyration were expressed[17] through R_{core} and R_{mic} as

$$R_{g1}^2 = \frac{3}{5} R_{core}^2 \tag{5}$$

$$R_{g2}^2 = \frac{3}{5} \frac{R_{mic}^5 - R_{core}^5}{R_{mic}^3 - R_{core}^3} \tag{6}$$

Table 1 summarizes the results obtained using two different approaches to SANS data. The first approach uses the Guinier analysis while the second is based on the assumption of the core/shell model. The latter approach failed for low degrees of neutralization. For α < 0.06, it was not possible to determine the core parameters reliably enough because they were sensitive to the choice of the q-interval used in the fitting. This indicates that the **PEHA−PAA** at low degrees of neutralization forms aggregates or irregular particles instead of simple core/shell micelles. As indicated by a decrease in M_w^{Guin} and R_g, ultrasonic treatment of the solution with α = 0 leads to disaggregation, but the resulting particles are not quite regular spherical micelles. It should be noted that the values of M_w^{Guin} and R_g are underestimated because no extrapolation to zero concentration has been made. Therefore, M_w^V and M_w^I are probably better estimates of the particle mass. Neutralization of the PAA shell is accompanied by considerable decrease in mass of the particles (by one order of the magnitude) and by narrowing size distribution. At full neutralization, the particles are probably spherical micelles with a core having mean radius of 4.7 nm and composed of about 40 PEHA oligomeric chains. The overall radius of the micelle was estimated to be 24 nm. As expected, due to concentration effect,

Scheme 1

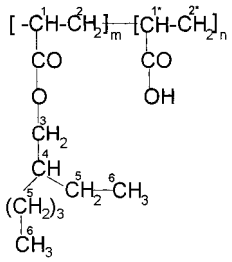

this value is lower than the results of NMR and DLS measurement.

Cumulative treatment of DLS data provided the value of hydrodynamic radius, $R_H = 28$ nm, with low dispersity of spherical objects. Approximately the same value of *rotational* hydrodynamic radius, i.e., 26 nm, was found by NMR (see below).

Effects of Physical Structure and the Correlated Motional Restrictions of the Micellar System on NMR Spectra. In the following section and throughout the rest of the paper, the NMR signals are assigned according to Scheme 1. The resonance of proton 4 forms a multiplet screened by other signals and is thus not detected in the spectra. The signals of the **PEHA** skeletal protons 1 and 2 mostly overlap with those of the analogous protons of **PAA** (1* and 2*) in molecular solutions of the copolymer. In the micellar state, signals 1, 2, 3, and 4 are broadened beyond detection unless the core is swollen by a good solvent.

Figure 3 compares NMR spectra of (i) **PEHA**−**PAA** aggregates and (ii) **PEHA**−**PAA** single micelles in D_2O with (iii) that of bulk **PEHA** at 330 K. Signal 6 of the methyl groups in **EHA** side chains in the bulk polymer is much narrower than those in both other systems although its polymer chains are about 18 times longer than those in the micelles or aggregates. Assuming normal behavior of **PEHA** chains in all systems under consideration, the higher polymerization degree in the bulk polymer should lead to a higher viscosity and, consequently, to a slower motion of methyl groups and thus to broadening of their NMR signals. Quite the opposite is observed.

In the bulk polymer, the methyl signal exhibits partial splitting (corresponding to the spin J-coupling to the neighboring methylene groups). At 330 K, the half-width $\Delta\nu_{1/2}$ of the signal is 14.6 Hz; i.e., it is mostly given by the *J*-splitting. In contrast, the corresponding signals in the micellar systems are substantially broader and exhibit asymmetry which will be the subject of further discussion.

Figure 4 compares the spectra of **PEHA**−**PAA** micelles with various degrees of neutralization of the **PAA** chains with NaOH. Dramatic change in the half-width of signals 5 and 6 brought about even by partial neutralization can be seen. As observed by SANS, the fully acidic form obtained by dissolution of the freeze-dried form in D_2O is perceptibly aggregated whereas even slight neutralization leads to gradual dispersion of the aggregates. The underlying change is, without doubt, the repulsion between the negative charges introduced into the **PAA** chains which counteracts the adhesion of the **PAA** chains. By the same logic, an increase in negative charge density due to a higher neutralization degree should lead to maximizing the distances along and between the **PAA** chains, i.e., to their extension and increasing rigidity with a higher neutralization degree.[7,8] This is exactly what is observed in the **PAA** part of the spectra where, in particular, the α-CH signal 1* is gradually shifted to higher field and, at the same time, smeared out into a very broad signal. Quite in contrast to these changes, however, the methyl signals 6 of the core **PEHA** are perceptibly, though less dramatically, narrowed.

Comparing the shapes of the signals of the micellar aggregates with those of both ultrasound and ionization dispersed micelles, a rather dramatic narrowing of the core signals (5 and 6) can be observed. The corresponding objects differ (i) in their volume and (ii) in the degree to which their micellar shells are interwoven and thus locally immobilized. The narrowing effect can thus be due either to a change in the frequency of their collective tumbling or, indirectly, to a relative increase in the local mobility of the **PAA** blocks. This can be discerned by the following observations.

To appreciate the role of the collective tumbling of the micelles, we increased the viscosity of the micellar solution by dissolving poly(ethylene glycol) (**PEG**, $M_n = 6000$) in the system. The effect of this can be seen in Figure 5 for two different neutralization degrees of the **PAA** chains. In accord with the above considerations, the core signals 5 and 6 are affected by viscosity rather more than those of the shell although no direct interaction of the core **PEHA** with the dissolved polymer could be imagined. Both signals are perhaps somewhat narrower (the difference in half-width being about 1.5 Hz) but strikingly less intense than the original ones. This effect is much more apparent in the case of a lower neutralization degree. By closer inspection, one can see that the broadest components of the signals are entirely missing in the case of high viscosity of the medium. Using MAS of 15 kHz on the same samples, the missing intensity can be restored. In other words, an increase in viscosity of the medium causes vanishing of the broader signal components due to their broadening beyond detection.

The increase in viscosity of the medium affects the collective tumbling rate of the micelle as a whole but could also influence (if to a lower degree) the local or semilocal mobility of the **PAA** chains in the shell and, indirectly, the mobility of **PEHA** chains attached to them. To discern this possible effect, we substituted the relatively light sodium ions in the fully neutralized form of **PEHA**−**PAANa** micelles in D_2O by tris(2-hydroxyethyl)ammonium ions which are much bulkier due to their hydration sphere and could be shown by ^{14}N NMR to be incomparably less dissociated. By inertial as well as steric factors, such substitution should decrease the mobility of **PAA** chains without influencing appreciably the tumbling rate of the whole micelle. The spectra are compared in Figure 6. As it can be seen, such substitution influences almost exclusively the signals of the shell (mainly an absolute intensity decrease due to the vanishing, i.e., excessive broadening of their broadest components), whereas the effect on the core signals is almost negligible.

The conclusion of these experiments is that the rate of the collective isotropic tumbling of the system (a micelle or a micellar aggregate) influences both the shape and intensity of the signals of the core **PEHA** blocks. In contrast to the micelles of low-molecular-weight surfactants,[18] this rate cannot be large enough to influence proton relaxation directly. It could be sufficient, however, to cancel (partly or completely)

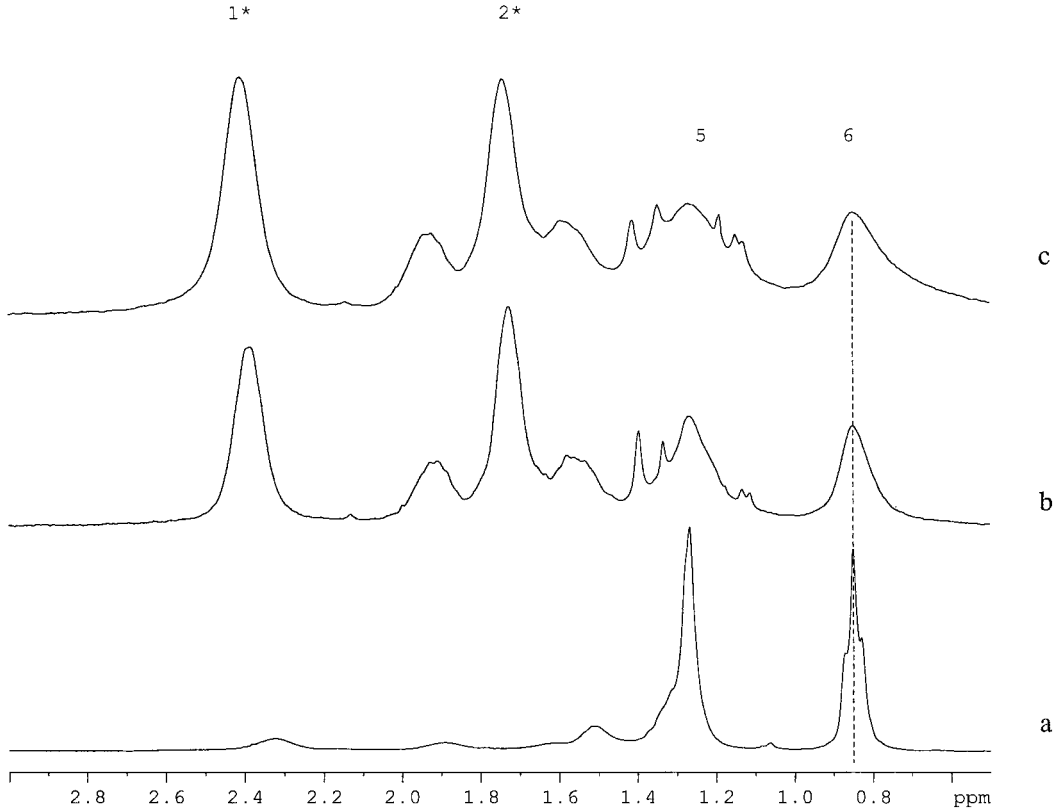

Figure 3. ^{1}H NMR spectra of (a) bulk **PEHA**, (b) **PEHA**−**PAA** single micelles, and (c) their aggregates at 330 K (in a and b, 0.5% w/w in D_2O).

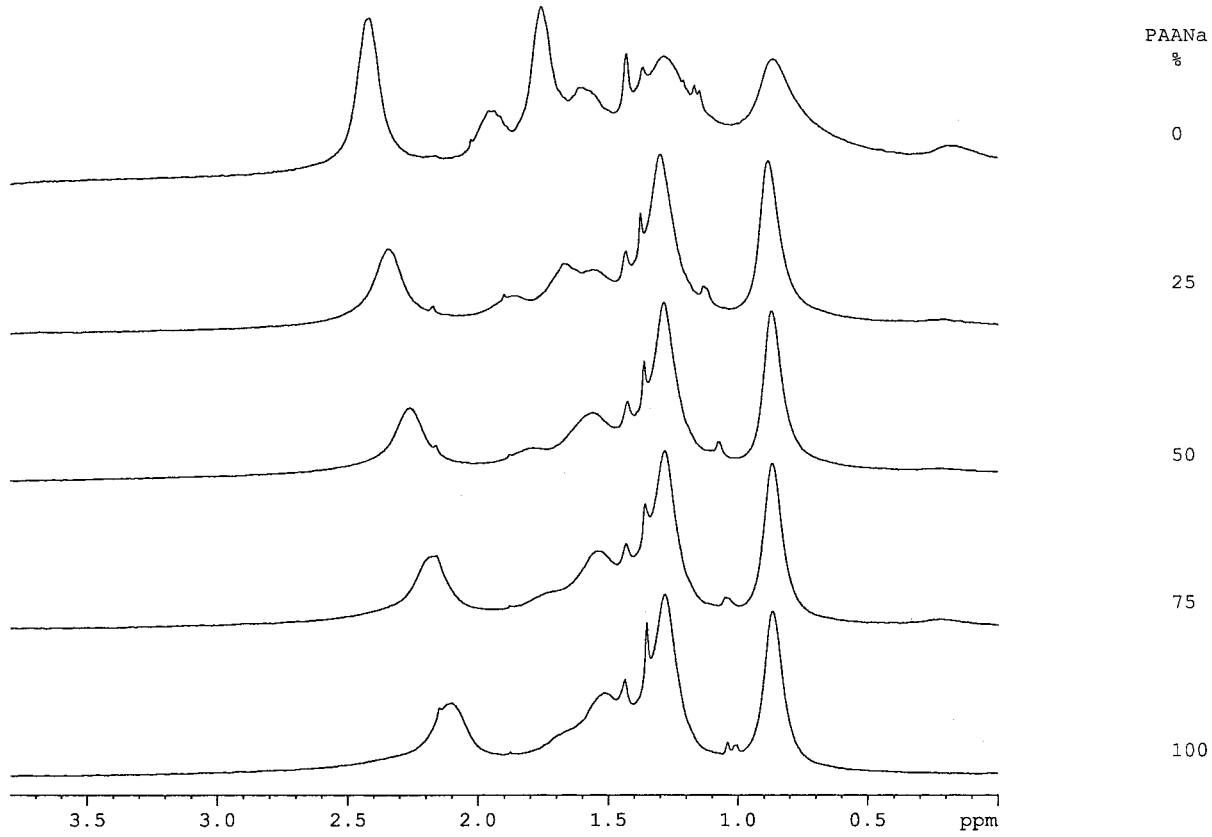

Figure 4. ^{1}H NMR spectra of **PEHA**−**PAA** micelles (0.5% w/w in D_2O) at different degrees of neutralization.

residual static dipolar interactions and/or shielding anisotropies resulting from partial restrictions of the local motions of some of the **PEHA** groups.

In full accord with this explanation, magic angle spinning is also effective in narrowing the signals. Figure 7 compares 200 MHz MAS NMR spectra of

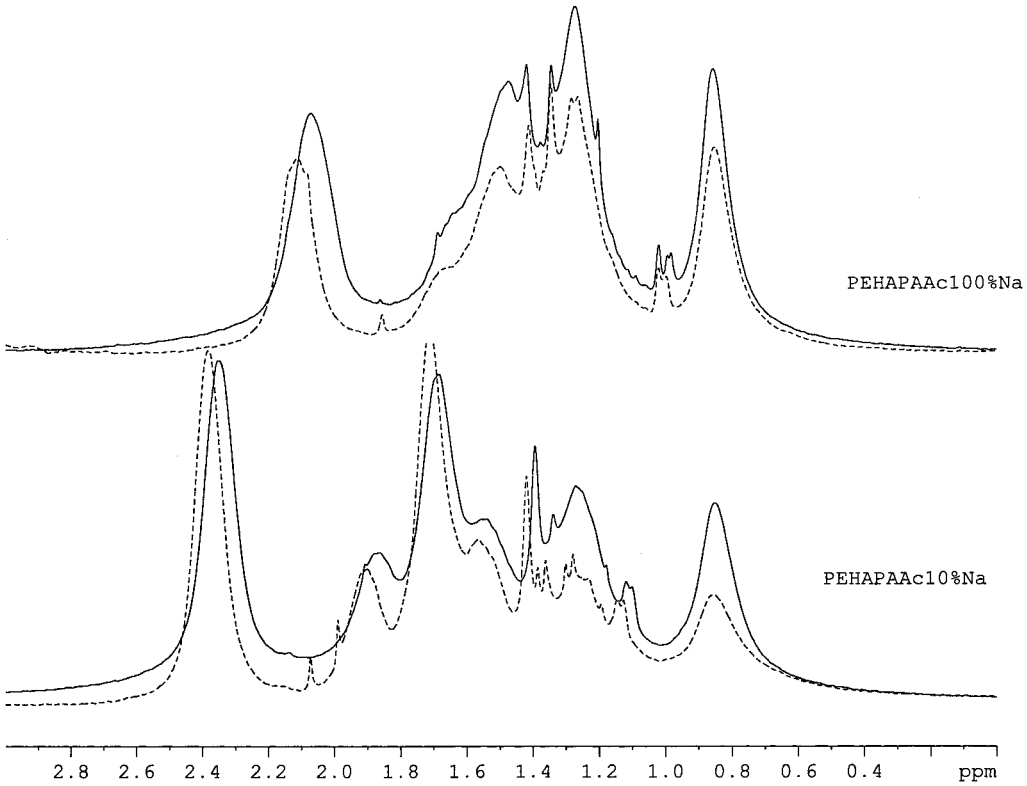

Figure 5. ^{1}H NMR spectra of **PEHA−PAA** micelles (neutralization degree 10 and 100% Na): (a) in pure D_2O (full line) and (b) in a 5% w/w solution of PEG 3000 (dashed) in D_2O (330 K).

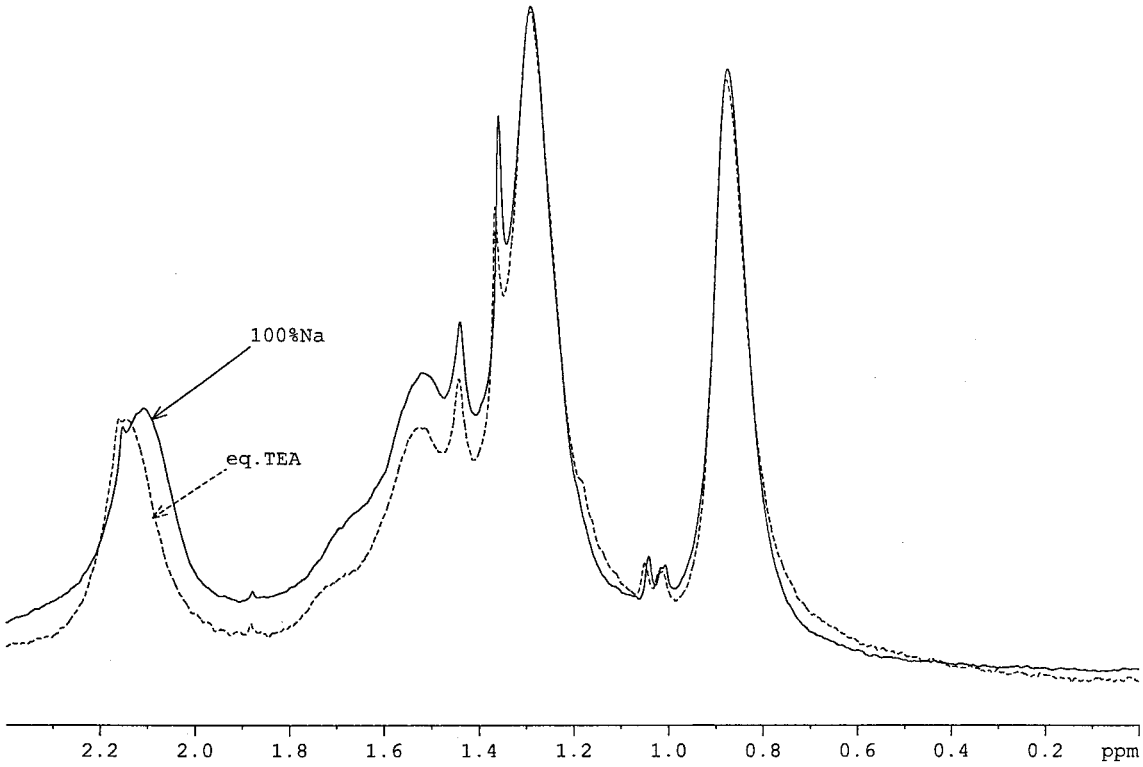

Figure 6. ^{1}H NMR spectra of **PEHA−PAA** micelles neutralized to 100% with (a) NaOH (full line) and (b) tris-(2-hydroxyethyl)-amine (dashed line) in in D_2O (330 K).

PEHA−PAA micellar aggregates under a gradual increase in the spinning frequency from 2 to 15 kHz at 320 K. The signals are gradually narrowed and increased in absolute intensity by MAS. The rotational side bands observable chiefly at lower spinning frequencies copy the structure of the main spectrum showing thus that all its signals contain components broadened by residual static dipolar interactions. Around a spinning rate of 10 kHz, both shape and intensity of all the main signals become very similar to those in the static spectra of the single micelles at the same temperature. It can thus be concluded that the relative broadening

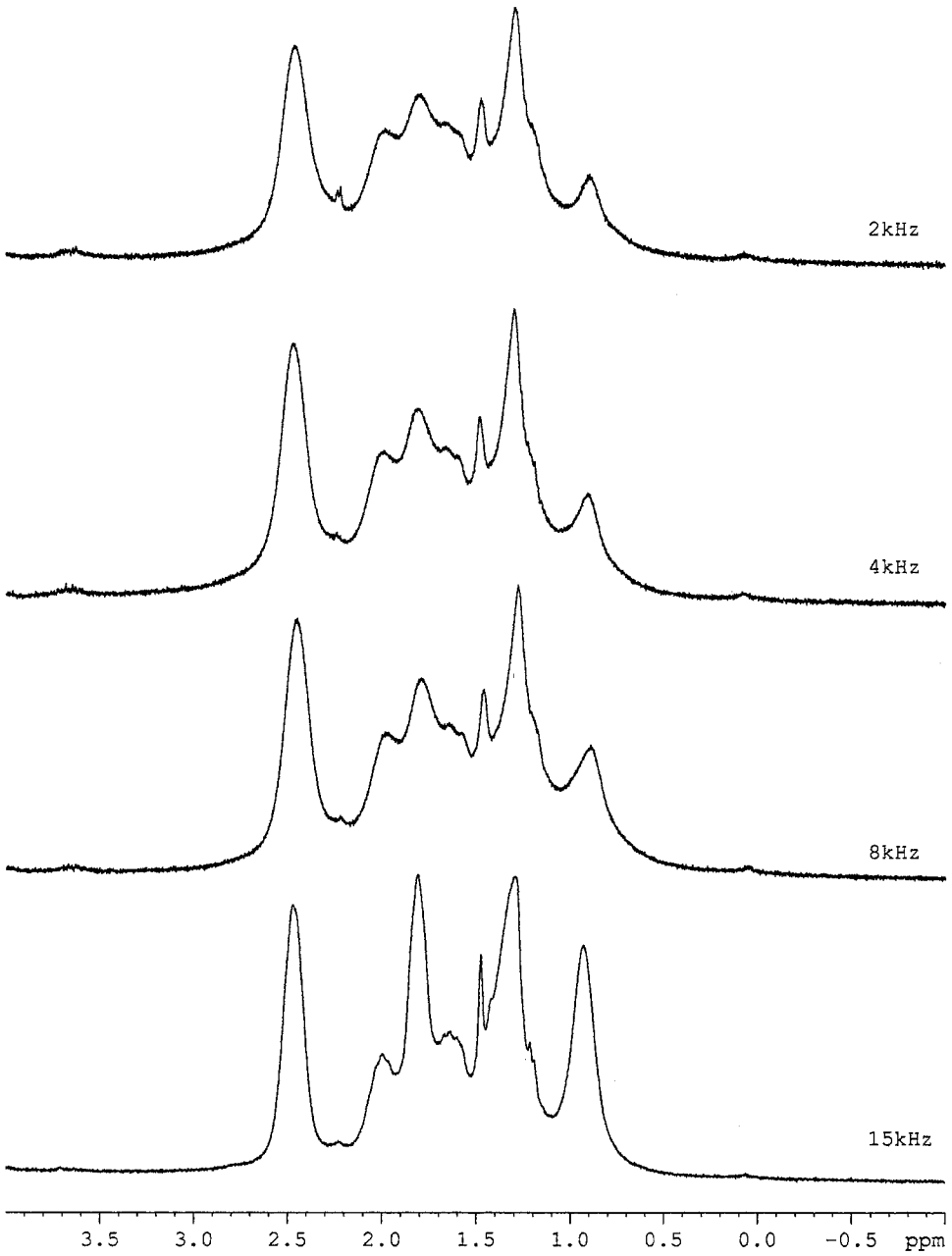

Figure 7. 200 MHz ^{1}H MAS NMR spectra of **PEHA−PAA** aggregates under different spinning frequencies at 320 K.

of the signals under micellar aggregation is due to the decreased overall tumbling rate. Bearing in mind that isotropic tumbling has an equivalent canceling effect on direct dipolar coupling as magic angle spinning, we can conclude that the isotropic rotational diffusion of single micelles should have the frequency of about 10 kHz. Using, as an approximation, the well-known Debye relation for the correlation time τ_r of rotational diffusion of a spherical object

$$\tau_r = 4\pi\eta R^3/3kT \qquad (7)$$

where η is the viscosity of the medium, k the Boltzmann constant, and T the absolute temperature, we can estimate the value of R about 26.3 nm which is in a very good agreement with theoretical expectations as well as with experimental scattering data.

Owing to the third power of R in eq 7, even quite small changes in R have a pronounced effect on the frequency of rotation and, consequently, on the importance of residual dipolar broadening of the corresponding NMR signals. In view of this, the larger tendency of more acidic **PEHA−PAA** micellar systems to aggregation and thus their lower mean tumbling rate should lead to a larger population of broader components in the corresponding 5 and 6 signals, detected either directly in the wings of the signal or indirectly (in the case of extreme broadening) by a decrease in the absolute signal intensity. Both cases are observed.

At 320 K, 15 kHz MAS increases the absolute intensity of the signal 6 in the proton spectrum of **PEHA−PAA** (neutralized to 25%) by about 62% whereas equilibrium swelling of the micellar core of the same system with chloroform, which removes most of the hindrances to local motions in the core,[8,10] produces a 38% relative increase in intensity of the same signal in the high-resolution spectrum. Clearly, even equilibrium swelling of the core with a good solvent cannot remove all the motional restrictions leading to extreme signal broadening.

The core signals are not only narrowed and increased by MAS. As seen in Figure 7, the higher spinning rate also leads to the decreasing asymmetry of signals 5 and 6. At 15 kHz, the signal 6 is almost symmetric and Lorentzian. An analogous loss of asymmetry can be observed in the static spectra under increasing neutralization degrees of the **PAA** shell (Figure 4). This effect cannot be explained solely by canceling the static dipolar interactions by either MAS or isotropic tumbling of the micelles. As shown above, the radius of the whole micelle (and consequently the rotational correlation time) is found by SANS to be approximately constant in the region from 20 to 100% of neutralization. A plausible explanation, however, is offered by magnetic shielding anisotropy.

As shown both in theory and experiment,[27] a spherical object (the micellar core in our case) with the radius ρ and magnetic susceptibility χ_s immersed in a medium with a different susceptibility χ_m induces in its surroundings (in contrast to its interior[28]) under the influence of a homogeneous magnetic field $\mathbf{H}_0$ an additional field of intensity

$$H_i = (4/3)\pi(\chi_s - \chi_m)\mathbf{H}_0 \langle 3\cos^2\vartheta - 1\rangle(\rho/r_i)^3 \quad (8)$$

(where ϑ is the angle of the director of the ith point with the vector $\mathbf{H}_0$ and r_i its length). Such field produces outside the sphere a relative chemical shift of a NMR signal $\Delta\nu_i$ which has a radial as well as angular dependence with a maximum value $\Delta\nu_{max} = 2\gamma H_0(\chi_s - \chi_m)$. Due to the $\langle 3\cos^2\vartheta - 1\rangle$ term in eq 8, $\Delta\nu_i$ can be canceled either by MAS or isotropic tumbling of the micelle. Taking the χ values -0.638×10^{-6} and -1.356×10^{-6} egs/mL for D_2O and hexane,[29] one obtains for protons at 300 MHz resonant frequency $\Delta\nu_{max} = 2692$ Hz, i.e., 8.975 ppm. Roughly a tenth of this value is observed. At the same time, approximately a third of the total absolute intensity of signal 6 corresponds to a population of relatively shifted signals in the purely acidic form of single micelles whereas an almost negligible fraction of the shifted signals 6 could be expected in the case of a sharp core−shell interface. These discrepancies can be explained when reflecting the SANS results. As shown in Table 1, the core radius found in the fully neutralized form is 4.7 nm whereas that in a purely acidic form (single micelles) is 2 nm larger, i.e., 6.7 nm. The only plausible explanation for such a large difference at a comparable size of the whole micelles is a partial entwining[8,10] of the interior segments of the **PAA** blocks with the exterior **PEHA** units under formation of a mixed interface. The thickness of such mixed layer must decrease with the increasing degree of **PAA** neutralization due to larger hydrophilicity and mutual repulsion of the ionized segments. This is shown by the SANS data and, in an entirely different way, by NMR: signals 2* and, in particular, 1*, corresponding to **PAA** backbone groups, are easily broadened beyond detection in the high-resolution NMR when the corresponding segments are relatively immobilized by entwining with the hydrophobic groups but can be revealed by swelling the micelle with a suitable solvent[8] such as $CHCl_3$. NMR finds a 39% relative increase in the absolute intensity of signal 1* after equilibrium swelling with $CHCl_3$ of the acidic micelles but almost none in the case of the fully neutralized ones. Considering the portion of the immobilized **PAA** in the acidic form and the corresponding core radius found by SANS, 25−30% of **PEHA** must be placed in the mixed **PEHA**−**PAA** interface. As the side groups 5 and in particular 6 are naturally more mobile than the **PAA** backbone groups, they can be observed even in the interface layer, their signals being variously shifted due to the shielding anisotropy produced by the inner **PEHA** core. The magnetic susceptibility difference between pure **PEHA** and its mixture with **PAA** can be expected to be substantially lower than that between **PEHA** and D_2O, hence giving the observed maximum shift of about 0.9 ppm. The only gradual symmetrization and narrowing of the signal 6 under increasing spinning rate in MAS shows that residual static dipolar interactions (which are less easily canceled by MAS) influence its shape. Consequently, the **PEHA** groups entwined in the mixed interface or placed near to it must be relatively restricted in their motion. If the effects of field anisotropy and dipolar broadening for the protons placed in the interface area are combined, signal 6 can be expected to be asymmetric due to its variously upfield-shifted and broadened components. In all cases analyzed, the signal could be approximated by a superposition of at least three (but probably many more) relatively shifted Lorentzians, the more upfield shifted ones being broader and less intense. Typical values (for 10% neutralization and 330K) of $\Delta\nu_{1/2}$ were 23, 30, and 83 Hz with intensities decreasing in the order 1.0:0.8:0.2. These half-widths correspond to T_2 values of 7.25, 5.38, and 1.93 ms, indicating thus a rather complicated functional form of the signal decay under T_2 measurement. This, again, is observed and the results will be discussed below.

Assuming a Lorentzian shape of the individual components of one signal (surely a rather crude approximation for the most restricted groups) but a distribution of transverse relaxation rates, one can expect the following development of the signal (both absolute integral intensity and shape) when increasing the pre-acquisition delay t:

$$I = I_0\sum 2w_i(0)\exp(-t/T_{2i})T_{2i}/[1 + 4\pi^2 T_{2i}^2(\nu - \nu_{0i})^2] \quad (9)$$

where $w_i(0)$ and ν_{0i} are the original population and resonant frequency of the ith component in the signal. Due to eq 9, the signal shape must change with growing pre-acquisition delay. This can be used for further exploration of the signal utilizing the well-known Carr−Purcell−Meiboom−Gill (CPMG) sequence as a kind of T_2 filtering. The results of such measurements (spectra after the cumulative pre-acquisition period of 10, 20, 30, and 40 ms) with **PEHA**−**PAA** aggregates and single micelles and with fully neutralized **PEHA**−**PAANa** micelles are shown in Figure 8. As one can see, the broadest and most magnetically shielded components are filtered off very quickly. The residues of signals 5 and 6 gradually shift in the downfield direction and converge to the position (and almost to the half-width) of the corresponding signals in bulk **PEHA**. As the interior of the micellar core is probably most similar to bulk **PEHA**, one can conclude that the upfield shifted and broadened signal components correspond to those parts of the **PEHA** blocks which are near to the core−shell interface. This is in full accord with the finding discussed above that the upfield shift and broadening must be due to shielding anisotropy and dipolar broadening on the core−shell interface. As a strong support

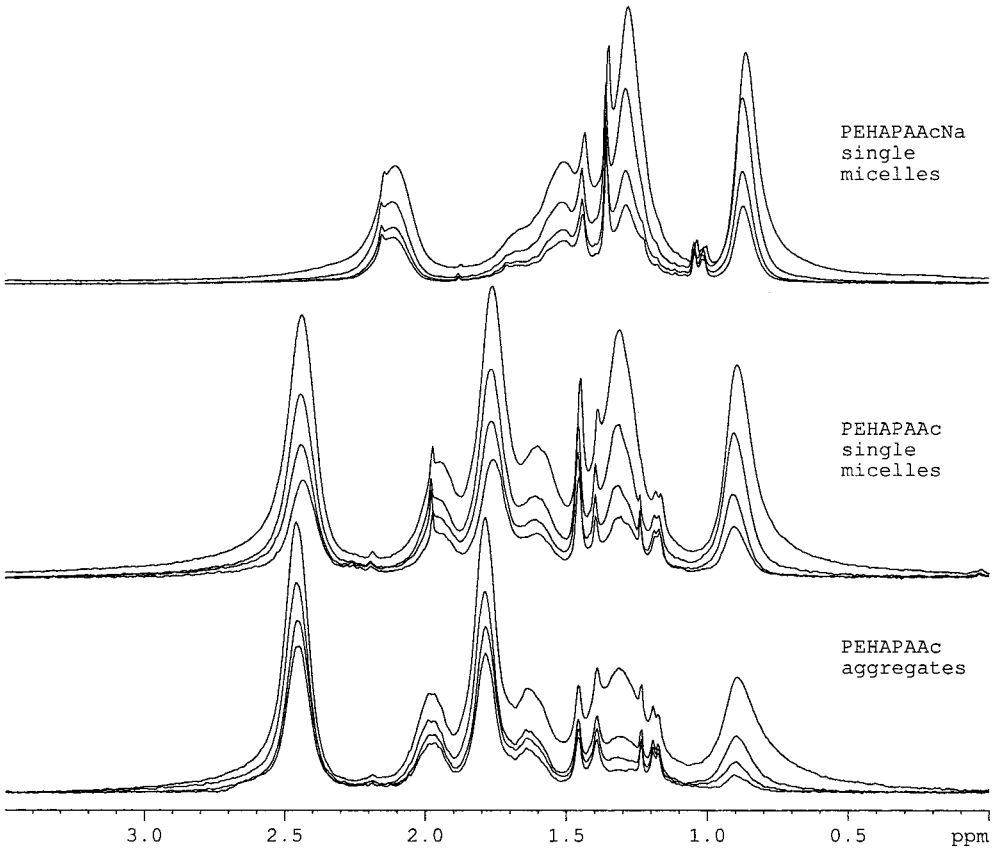

Figure 8. ^{1}H NMR spectra of **PEHA**−**PAA** micelles, their aggregates or their 100% Na salts after 10, 20, 30, and 40 ms of T_2 filtering.

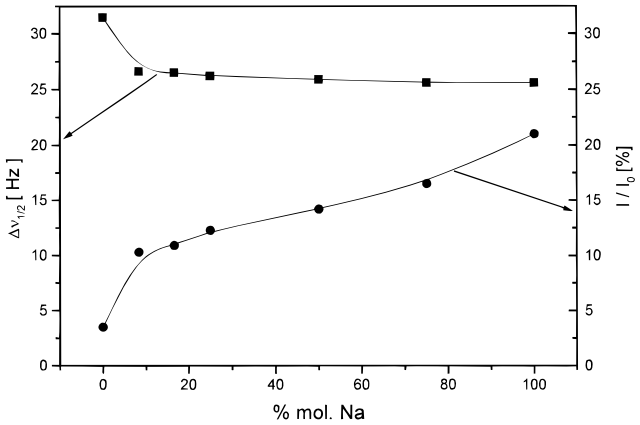

Figure 9. Residual half-width and intensity of signal 6 in ^{1}H NMR spectra of **PEHA**−**P**AA after 40 ms of T_2-filtration in dependence on the degree of neutralization.

for this conclusion, real time NMR observation of the change of the signal shape under gradual diffusion of chlorobenzene (which is known to have a steep diffusion profile[10]) into the micellar core shows that the broadest high-field components of the signal are narrowed in the earliest stages of the core swelling.

The population of the narrowest components (obtained either by a deconvolution of the original signal or from the absolute intensity of the residual signal after a fixed period of T_2-filtering) is quite different in each of the demonstrated instances. Figure 9 shows the linewidths of the near-Lorentzian signals obtained after 40 ms of T_2-filtration (using $\tau = 1$ ms) and their integral intensities relative to the original signals, for micelles with different neutralization degree. Clearly, the relative population of the narrowest component increases with increasing ionization of the shell whereas its half-width rapidly converges at first and remains constant at higher ionization degrees.

Table 2. Longitudinal Relaxation Times T_1 (in s) of Main Signals in Bulk PEHA and a 0.5% Micellar Solution of PEHA−PAA and PEHA−PAANa at 330 K

	PEHA	PEHA−PAA	PEHA−PAANa
1[a]		0.419	0.364
2[a]		0.287	0.292
5	0.576	0.559	0.495
6	0.632	0.607	0.593

[a] Ultrasonic treatment.

To summarize the above findings, the existence of motional hindrances and partial restrictions both in **PEHA** and **PAA** units, increasing up to relative immobilization in the vicinity of the core−shell interface, are strongly indicated by the NMR spectra.

NMR Relaxation and the Chain Mobility in Single Micelles. We have studied all three main types of NMR relaxation in our systems, i.e., longitudinal, transverse and rotating frame relaxation. Table 2 shows T_1 values for the main signals in bulk **PEHA** and 0.5% D_2O **PEHA**−**PAA** micellar solutions in both neutralization extremes at 330 K. In this case, the relaxation curves appear to be monoexponential if processed in the intensity mode (also clear signs of polyexponentiality can be observed if the signal areas are compared) and there appears to be no striking difference in relaxation rates in the bulk polymer, and the corresponding block in the micellar core.

In contrast to this, rotating frame and, in particular, transverse relaxation show both larger differences and

Table 3. Statistical Weights and Corresponding Transverse Relaxation Time Constants (in s) for the Main Components of Chosen Signals in Micellar PEHAPAA or PEHAPAANa (0.5%w/w in D_2O at 330 K)

	PEHAPAA				PEHAPAANa			
	1[a]	2[a]	5	6	1[a]	2[a]	5	6
w_1	0.079	0.086	0.117	0.113	0.247	0.219	0.155	0.140
w_2	0.438	0.442	0.618	0.611	0.363	0.399	0.618	0.625
w_3	0.483	0.472	0.265	0.276	0.390	0.382	0.227	0.235
T_{21}	0.004	0.007	0.006	0.007	0.003	0.003	0.002	0.002
T_{22}	0.015	0.021	0.011	0.012	0.014	0.015	0.008	0.009
T_{23}	0.169	0.122	0.041	0.042	0.126	0.100	0.042	0.048

[a] Ultrasonic treatment.

deviations from monoexponentiality. The respective T_2 values of signals 5 and 6 in the bulk **PEHA** at 330 K are 0.057 and 0.063 s, exhibiting large difference from the corresponding T_1 values shown in Table 3. These signals are the only ones at hand for the study of the local mobility in **PEHA**−**PAA** micellar cores, the others being broadened or obscured by the signals of the **PAA** shell (1* and 2*). The corresponding methyl (6) and methylene (5) groups are not ideal probes into chain mobility as their transverse relaxation is known to be complicated both by motional anisotropy as well as spin−spin coupling and, in addition, their separation by six to eight single bonds from the backbone usually makes them motionally almost independent of it. There are strong arguments, however, for a closer inspection of their relaxation behavior: (i) in a wide range of micellized amphiphilic block copolymers in water, **PEHA**−**PAA** and its salts appear to be the only one (except poly(propylene oxide)-poly(ethylene oxide) copolymers) exhibiting NMR signals of the core; (ii) according to the above-reported evidence, the motion of these groups is partly restricted or strongly hindered in the micellar core and thus correlated, partly at least, with the motion of the backbone.

It is well-known that the transverse relaxation measurement of a spin-coupled nucleus offers several problems, the most important ones being (i) the modulation of the spin−echo by spin coupling and (ii) a contribution of spin coupling to the transverse relaxation rate, in particular if *J*-coupling is periodically changed by conformational change. In our case, the spin coupling between protons 5 and 6 appears to be diminished to less than 3 Hz according to *J*-resolved 2D spectra. Theoretical simulations using the values in Table 2 and 3 Hz as the value of *J* indicate almost negligible influence of *J*-coupling on our results. To verify this conclusion experimentally, we measured the transverse relaxation of protons 6 with and without selective decoupling of protons 5. The corresponding decay curves were identical within experimental errors.

As shown by many authors, recently in two excellent theoretical studies by Brereton,[19,20] NMR transverse relaxation in a motionally restricted polymer chain can be expected to adopt a nonexponential algebraic form. Equation 9 clearly cannot hold in the cases where the motions of individual groups along the chain are strongly correlated with each other and with the motion of the whole chain. In our case, protons 5 and, in particular, 6 belong to end groups of normally very flexible side chains and their motions thus should be statistically almost independent of the conformational modes of the main chain. If this reasonable assumption were not fulfilled, the NMR signal would correspond to a *convolution* of two or more Lorentzians rather than a *sum* of

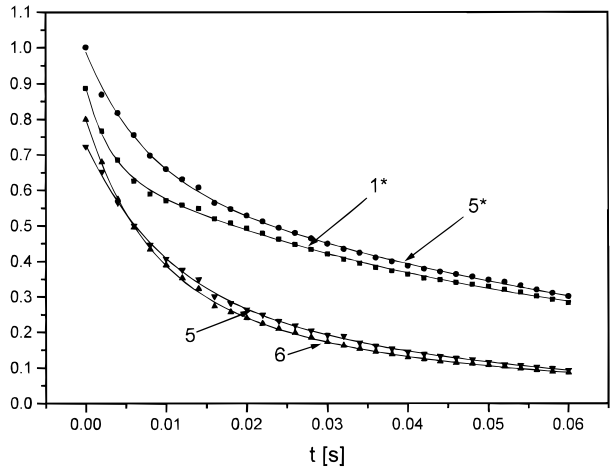

Figure 10. Transverse relaxation of the NMR signals 1*, 2*, 5, and 6 of **PEHA**−**PAA** single micelles (0.5% in D_2O, 330 K).

them. T_2-filtration experiments reported above indicate that the latter is mostly the case in our system; i.e., the system can be viewed as a collection of statistically independent groups with various mobilities, and eq 9 can be used as a viable approximation to the actual relaxation behavior.

We have studied two types of motionally sensitive relaxation: transverse relaxation (T_2) using CPMG sequence, making at least five independent measurements, each with five different delays between the refocusing pulses ranging from 0.4 to 1.6 ms, and for extremely short relaxation times, rotating frame relaxation ($T_{1\rho}$). The sequence of 16 or 32 spectra from each measurement was then analyzed (i) by an intensity and area fitting by a mono-, bi-, tri-, and tetraexponential function using three different algorithms and (ii) partly by a sequential signal shape analysis using eq 9. An example of the transverse relaxation decay for **PEHA**−**PAA** (single micelles) at 330 K is given in Figure 10. None of the observable signals decays monoexponentially but bi- and in particular triexponential functions fit the curves tenably. The same measurements were done for signal 6 using the saturated spin−echo method with a selective continuous-wave saturation of signal 5; the transverse relaxation of signal 6 was, within experimental errors, the same as in the normal CPMG measurement.

Evidently, the resonances 5 and 6 are effectively decoupled by signal broadening.[32] This can be utilized for yet another check of the assumption implicit in eq 9 that the polyexponentiality of the transverse relaxation of resonance 6 is due to a distribution of relaxation rates of the protons in differently placed methyl groups rather than to correlation of motion along the polymer chain.[19,20] In an effectively isolated methyl group, the only spin order available for second and third rank spin tensors and the corresponding higher order coherences is the dipolar one. It has been shown[35,36] that the necessary condition for the multiple quantum coherences to be formed by the appropriate pulse sequence in such a system is a nonzero value of the cross-correlation terms between the same group due to some restrictions in their rotation-wobbling motion. We thus measured intensity optimized zero-, double- and triple-quantum-filtered ^1H NMR spectra of **PEHA**−**PAA** and found that the relative intensity of signal 6 in them is lowered to 13, 10, and 8%, respectively. The relaxation decay curves corresponding to the zero and double coherence are

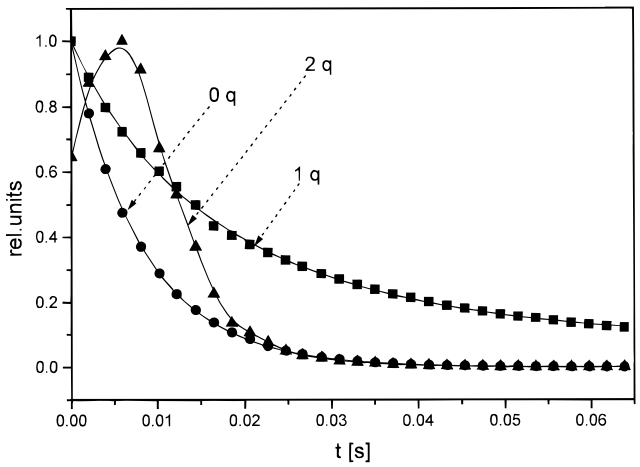

Figure 11. Comparison of transverse magnetization (1q), zero quantum (0q) and double quantum (2q) relaxation curves of the protons 6 in **PEHA**−**PAA** single micelles (0.5% in D_2O, 330 K).

compared with that of the ordinary transverse magnetization (or single quantum coherence) in Figure 11. The zero-quantum decay is expectedly monoexponential, the corresponding T_{ZQ} being 9.6 ms. By a fitting procedure, the value of T_{DQ} is about 8.2 ms. To exclude any possible influence of residual spin coupling, the same experiments were repeated with selective decoupling of protons 5, again with identical results within experimental errors. As the zero-quantum coherence is expected[36] to behave very much like the transverse magnetization except its low sensitivity to magnetic inhomogeneity, we can conclude from these experiments that merely a small part (about 10%) of the methyl protons in **PEHA** blocks experience a marked motional restriction leading to both production of multiple quantum coherence and fast transverse relaxation in the corresponding experiments. Considering this finding in combination with the evolution of signal shape and position in the T_2-filtered experiments reported earlier, we can be reasonably sure that the polyexponentiality of the transverse relaxation decay is mainly due to a distribution of relaxation rates.

The cumulative mean results obtained by fitting a triexponential function to intensity and area transverse magnetization decays in the span 0−0.16 s for two neutralization extremes, i.e., fully acidic and fully sodium-neutralized **PEHA**−**PAA**, are given in Table 3. The scatter of actual values obtained using different fitting algorithms, initial guesses or experimental point selections reached up to 39% relative to the respective mean value. In addition, the values of $T_{1\rho}$ obtained when measuring with extremely short decay times were much lower than those of the shortest component (T_{2i}) of the triexponential fit to the transverse relaxation, although quite the opposite could be expected. When inspecting the results closely, we noted that the results systematically depend on the time region spanned by the evaluated experimental points. Evidently, our systems offer a much more complicated distribution of relaxation times which cannot be handled effectively by triexponential fitting but which can be, partly at least, reconstructed using the following method: five different sets of 32 points (each reproduced at least three times) were obtained using τ delays from 0.4 to 1.6 ms, 16 subsets of 16 points were selected from each choosing the first to sixteenth, second to seventeenth, etc., point, and each subset was fitted by a triexponential decay function. The

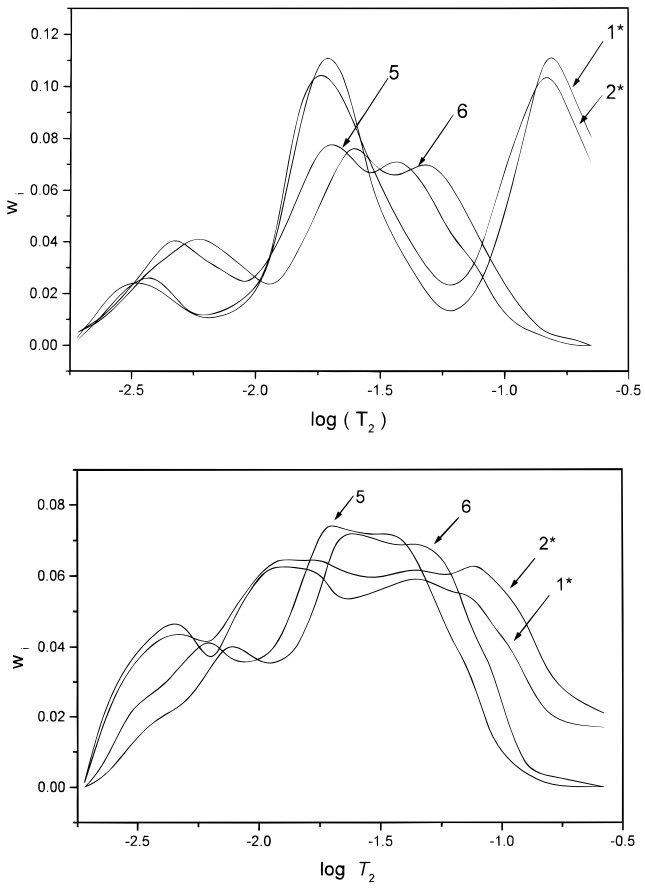

Figure 12. Reconstructed spectra of transverse relaxation time constants T_{2i} of signals 1*, 2*, 5, and 6 for (a) **PEHA**−**PAA** and (b) **PEHA**−**PAANa** (100% of neutralization).

amplitudes of each T_{2i} value obtained in such way were renormalized and collected in a distribution graph which is given in a semilogarithmic form in Figure 12a,b for the same neutralization extremes, i.e., **PEHA**−**PAA** and **PEHA**−**PAANa**. These graphs surely do not reproduce an *exact* distribution of relaxation times but they give some insight into the relaxation dynamics and thus mobility of the system.

The behavior of **PAA** signals 1* and 2* is perceptibly different in Figure 12a,b. In the acidic form, there appear three broad peaks which should correspond (cf. refs 7−9) to three regions of the **PAA** block having markedly different segmental mobility: that directly attached to or imbedded in the core−shell interface, the intermediary region where the **PAA** chains are partly entwined, and the relatively free moving part on the rim of the micelle. In **PAANa**, according to Figure 12b, the T_2 distribution is much more monotonic and shifted to lower values, i.e., lower mobility. This is in full accord with the generally accepted idea of a more pronounced stiffness of an ionized polyelectrolyte and, therefore, not very surprising.

An interesting behavior is exhibited by the two observable signals 5 and 6 of the **PEHA** block in the micellar core, however. As seen in Figure 12a,b, the distribution has two to three maxima, that corresponding to lowest T_2 being more broader in the case of micelles in the acid form of the shell. We have seen above in the T_2-filtering experiments that the slow relaxing components of signals 5 and 6 are magnetically most similar to bulk **PEHA**; in the analysis of the asymmetry of these signals, we have shown that the

Table 4. Statistical Weights and Corresponding Transverse Relaxation Time Constants (in s) of the Main Components of Signal 6 in Micellar PEHAPAA with Various Neutralization Degrees before and after Inserting PEHA into Its Cores (D_2O at 330 K)

	0%		25%		50%		75%		100%	
	before	after	before	after	before	after	before	after	before	after
w_1	0.079	0.053	0.086	0.062	0.117	0.083	0.113	0.079	0.247	0.103
w_2	0.438	0.310	0.442	0.314	0.618	0.314	0.611	0.320	0.363	0.294
w_3	0.483	0.637	0.472	0.624	0.265	0.603	0.276	0.601	0.390	0.603
T_{21}	0.004	0.006	0.007	0.009	0.006	0.008	0.004	0.007	0.003	0.006
T_{22}	0.012	0.019	0.009	0.011	0.011	0.019	0.010	0.020	0.009	0.018
T_{23}	0.042	0.062	0.038	0.049	0.057	0.062	0.052	0.060	0.048	0.059

very fast relaxing signal components correspond to the groups relatively immobilized in the interface region. From this, it can be concluded that the fast relaxing part of the present distribution should correspond to the **PEHA** region directly attached to the interface whereas the other two (or more) slower relaxing and more populated parts are probably those of the inner parts of the core. It has to be pointed out that even the slowest component included into this distribution has a T_2 value slightly lower than that of the corresponding signal in *bulk* PEHA at the same temperature whereas the fastest one has T_2 about 20 times shorter. As the cohesive interactions between the **PEHA** chains can be expected to be the same in the bulk polymer and in the micellar core, such outstanding differences between the respective mobilities must be due to the effect of the core−shell interface.

The units placed near to the core−shell interface (or forming a part of it in the acid form) must be restricted in their motion directly by the penetration resistance of the surrounding hydrophilic medium and indirectly by the resistance of the core itself against the correlated penetrations of the nearest units of the shell. This can be seen from the difference between the acid **PEHA**−**PAA** and its fully neutralized form: although the fast part of distribution of the latter lacks the extension to very short relaxation times (due to the absence of the mixed interface layer), the fraction of groups with $T_2 <$ 0.01 is perceptibly larger. The motions of the groups at the interface or near to it appear to be hindered to such extent that their signals apparently can be observed only due to the collective motion of the whole micelle. This is discussed in a semiquantitative way below in the Dynamic interpretation of NMR results.

Relaxation in Micellar Cores Swollen by Bulk PEHA. In the previous paragraph, we have shown that **PEHA** groups placed near the core−shell interface have distinctly hindered motions. Even groups placed in the interior of the core, however, have a mobility lower than those in bulk **PEHA**. This effect could be due to (i) the correlation of motion of the farther parts of the chain with those attached to the interface, (ii) the mere confinement of the chain in the restricted space of the core, or (iii) specific effects such as relative compression of the core by the surrounding water. Some insight into this problem can be achieved by the study of micellar cores containing **PEHA** chains unattached to the interface. Such systems were obtained by equilibrium swelling of the micellar cores with **EHA** and subsequent γ-irradiation (dose 2 kGy) induced polymerization at 295 K. It has to be noted that the equilibrium amount of **EHA** swollen into the core depended markedly on the ionization state of the shell, changing from 0.892 (fully acidic **PEHA**−**PAA**) to 0.568 (fully neutralized **PEHA**−**PAANa**) **EHA/PEHA**. No monomer escaped from the micelles during polymerization except in the case of neutralization degrees less than 10% where part of the monomer separated and formed an insoluble polymer. After correction for this loss, the added-**PEHA**/core-**PEHA** spanned the region from 0.782 to 0.568. SANS data for the same samples gave the values of this parameter for various procedures in the interval 0.9−0.7. No dependence on the degree of neutralization was found.

To ensure that no cross-linking or grafting induced by the relatively mild irradiation dose complicated the relaxation behavior, micelles of the same type but without any **EHA** were irradiated with the same dose and their relaxation measured at the same conditions. The results are given in Table 4. Dilution of the core chains with free **PEHA** leads to a merely slight change in the individual T_{2i} constants in the triexponential fit but to a perceptible change in their relative weights. **PEHA** blocks cannot be rigorously distinguished from unattached **PEHA** chains in this analysis. Nevertheless, the results indicate that the groups in the free **PEHA** chains as well as the remote groups in **PEHA** blocks have a mobility somewhat increased in these systems but still lower than those in bulk **PEHA**. It is safe to conclude that the mere confinement of the chain in the core leads to a slight decrease in its mobility. We are not able to decide, however, whether this effect is due to a mere spatial restriction or to some additional factors.

Dilution of the core with free **PEHA** clearly does not substantially alleviate the restrictions in the mobility of the interface-near **PEHA** blocks. This can be seen from the fact that the fraction of the fast relaxing groups (relative to the fraction of interface-attached **PEHA** blocks) remains approximately unchanged. Considering the increase of the interface area of the core, one can conclude that the main cause of the distinct relative immobilization of these groups both in the intact as well as **PEHA**-swollen micelles is the resistance of hydrophobic and hydrophilic groups against their mutual exchange.

Conclusions about the Mobility of Groups in a Micellar Core. As briefly shown in the Appendix, there is a complex relation between the relaxation rates found in our experiments and the correlation times of the various motions of the individual nuclei and the corresponding groups. According to the SANS and DLS data on the hydrodynamic radiuses, the main complicating factor, namely the tumbling of the whole micelle, should have approximately the same impact in all inspected cases, however. For differently placed groups in the same micelle, it is exactly the same (the factor is angular not radial). The distribution of the T_2 can thus be considered to be a direct reflection of the distribution of corresponding mobilities.

We can conclude that there are at least three main types of the observable groups in the micellar core

characterized by perceptibly different mobility. According to our analysis, these types differ more in the way the groups are connected to the interface than in their radial placement in the core. These types correspond to (i) the groups attached to the core−shell interface or to the next several units of the **PEHA** block, (ii) the groups relatively near to the interface due to their position in the **PEHA** block or to their statistical position, or (iii) the groups in the interior of the core. Type i is formed in about 10% (depending on the ionization state of the shell) and is characterized by a strongly hindered and spatially partly restricted motion ($\kappa = \tau_i/\tau_b \approx 20$, τ_i and τ_b being the correlation times of the given type and the analogous groups in the bulk polymer, respectively). Type ii is formed by most (about 60%) of the groups; the corresponding motion is hindered to a considerable degree still ($\kappa \approx 11$). Type iii forms the remainder and the mobility of the corresponding groups is comparable (if lower) to that of bulk **PEHA** ($\kappa \approx 2$). These conclusions appear to be in some agreement with Monte Carlo simulations of the chain behavior in a spatially restricted area such as a micellar core (cf., e.g., refs 21 and 22).

The source of the motional restrictions in the area of the core−shell interface is the entwining of the respective hydrophilic and hydrophobic groups. In the absence of any important interface layer, the source of the motional hindrances and restrictions in the core can be of three different types: (i) the resistance of both the hydrophilic shell and the hydrophobic core groups to a lateral exchange (a *toposelectivity* effect), (ii) the spatial restriction given by the outer profile of the core (*encasement* effect), and (iii) the osmotic pressure of the interface water molecules squeezing the surface layers of the core (a *hydroexclusivity* effect). According to our results, the impact of these effects on the mobility of the observed groups decreases in the order i to iii.

Acknowledgment. The authors thank the Grant Agency of the Czech Republic for its Grants 203/95/1319 and 203/96/1387 and the Academy of Sciences of the Czech Republic for its financial support given under Grant K2050602/12.

Appendix: Dynamic Interpretation of the NMR Spectra and Relaxation Measurements

The above-reported NMR results reflect at least four different dynamic factors: (i) the essentially isotropic motion of a side group in the quasi-isotropic medium of the core interior, partly hindered by its effective viscosity; (ii) the hindrances of the same motion due to its correlation with the motions of the chain backbone; (iii) the relative restrictions of the groups, in particular those at the interface, leading to a spatial anisotropy of their motion and resulting in residual near-static dipolar interactions; (iv) the effects of magnetic shielding anisotropy and field inhomogeneity at the core−shell interface. All these factors lead to an increase in transverse and, to a lower degree, longitudinal relaxation rate but their relative impact is different: factors iii and iv, as such, are much more effective in signal broadening, with factor iv additionally causing signal asymmetry, but this can be canceled by sufficiently fast MAS of the sample or isotropic tumbling of the micelle.

The expression of all these factors is relative in each case and clearly depends both on the local mobility of the group and the collective motion of the whole micelle. This calls for at least a semiquantitative dynamic model which could express the weight of these factors in a given case. As we are dealing with a complex system where a rigorous treatment is hardly possible, we adopt a pragmatic approach similar to that used with micelles of low-molecular-weight surfactants or large macromolecules (cf. refs 18−22).

We start with the observation that, in a dilute solution of **PEHA** in chloroform at 330 K, the methyl groups 6 in contrast to the CH groups 1 almost fulfill the "extreme narrowing" condition; i.e., their motion is in effect isotropic and relatively free although dependent on many cooperative motions. In bulk **PEHA**, as already stated, there is already a marked difference between T_1 and T_2 of these groups, suggesting a nonvanishing correlation of the motions of the side groups with those of the polymer backbone due to the increased viscosity of the medium. The motions are thus somewhat hindered but no signs of any spatial restrictions or distribution of relaxation times or chemical shifts could be found. When going over to the **PEHA** groups in the micellar core, we were able to prove both motional *hindrances* in most of them, but also some spatial *restrictions* and *shielding anisotropies* (in some of them at least). Whereas the relaxation effects of the mere motional hindering by an increased effective viscosity of the surroundings cannot be removed by isotropic tumbling of the whole micelle or by MAS of the sample at any realistic frequency, the latter ones can and do, in part at least, as shown above. We thus can use the formalism of the "two-time" model,[18,19,31,32] i.e., we express the transverse relaxation rate R_{2i} of the ith species as

$$R_{2i} = (1 - S_i^2)\,\xi_{if} J_{if}(\omega) + S_i^2\,\xi_{is}\,J_{is}(\omega) \qquad \text{(A1)}$$

where S_i is the *order parameter* (defined irrespective of the collective tumbling of the micelle, i.e., as static), $S_i = \langle 3\cos^2\vartheta - 1\rangle/2$, ϑ being the angle between the z-axis of the diagonalized tenzor of the main relaxation interaction of the ith nucleus (e.g., the connector with the nearest spin in the dipolar relaxation) and the vector of the main magnetic field, $\boldsymbol{H}_0$, and the brackets mean the average of the quantity in the NMR relevant time window (cf. refs 31 and 32) ξ and J are the corresponding interactions and reduced spectral densities. $J_{if}(\omega)$ refers to the fast (quasi-isotropic) movement, in our approximation independent of that of the whole micelle, i.e.

$$\xi_{if} J_{if} = (1/20)(\mu_0/4\pi)^2(\gamma^2 h/r_{ij}^3)^2\,[3J_i(2\omega_0) + (15/2)J_i(\omega_0) + (9/2)J_i(0)] \qquad \text{(A2)}$$

for predominantly dipolar relaxation, whereas $J_{is}(\omega)$ expresses the motion under *spatial restriction* which leads to *residual static dipolar* or *shielding anisotropy* broadening (i.e., relaxation rate increasing). In the usual two-time approach, J_{is} corresponds to the rotational diffusion of the micelle itself, i.e., for isotropic motion, $J_{is}{}^i = 2\tau_r/[1 + (\omega\tau_r)^2]$. In our case, τ_r is about 3.2×10^{-5}; hence, the collective tumbling *as such* cannot play any direct role in the time window of a 300 MHz resonance. It can, however, significantly affect the residual dipolar or shielding anisotropy broadening in the region 10^2−10^4 Hz. In an acceptable approximation, we propose J_{is} to be a Fourier transform of a convolution of two correlation functions, $G_r(t) \otimes G_s(t)$, where $G_r(t) = \exp$-

$(-t/\tau_r)$, which is that of the isotropic tumbling, and $G_s(t)$ is allowed to be the correlation function of the sum of various types of residual broadening, $G_s(t) = \sum_j G_{ij}s(t)$. Using the second moment approximation to the whole system of residual static broadenings, we can express (in some analogy to earlier works[23−26]) J_{is} by

$$J_{is} = \int_{-\infty}^{\infty} \exp(-i\omega_0 t) \exp[-\omega_{2i}{}^2 \int_0^t (t-\tau) \times \exp(-|\tau|/\tau_r)\, d\tau]\, dt \quad \text{(A3)}$$

which can be, in the region of practically important frequencies, tenably approximated by the function[33,34] $\xi_{is}J_{is} \approx \omega_{is}{}^2 \tau_r{}^2[\exp(-t/\tau_r) - 1 + t/\tau_r]$

In a radical simplification, the relaxation rate of the ith species can thus be expressed as

$$R_{2i} = (1 - S_i{}^2)\, R_{2i}{}^f + S_i{}^2\, F(R_{2i}{}^s, \tau_r) \quad \text{(A4a)}$$

$$= (1 - S_i{}^2)\, \xi_{if} J_{if} + S_i{}^2 \xi_{is} J_{is} \quad \text{(A4b)}$$

where $R_{2i}{}^f$ and $R_{2i}{}^s$ are the relaxation rates corresponding to the spatially unrestricted and restricted motion, respectively, and F is the function expressing the role of $R_{2i}{}^s$ under the given averaging collective motion (MAS or isotropic tumbling).

In this model, $R_{2i}{}^f$ reflects the hindrance of motion by the effective viscosity in the absence of spatial restrictions, S_i and $R_{2i}{}^s$ reflect the restrictions of motion which can be only temporal but must be effective in the NMR time window. This mutual entwining of different kinds of motional hindrances (corresponding to relatively different energy barriers) in our model reflects the physical reality. Given the same τ_r for the whole micelle and supposing, for simplicity, $R_{2i}{}^f$ to be constant for all groups in the micellar core, a *perceptibly* increased value of $R_{2i} = 1/T_{2i}$ for a given unit has to correspond to relatively larger value of S_i or/and $R_{2i}{}^s$; in both cases, relative motional restrictions are indicated. On the other hand, if the second term in eq 13 is driven to zero by rapid micellar tumbling or MAS, the increased R_2 (relative to bulk polymer) has to be given by increased $R_{2i}{}^f$, i.e., by an increased effective viscosity of the material. The mutually interwoven factors of relaxation can thus be, at least in principle, disentangled and interpreted. Using the above obtained T_{2i} distributions and the value of S_i monotonically radially increasing from 0.1 to 0.35 (the largest being at the interface), the simulated relaxation change of the shape of signal 6 in **PEHA−PAA** and **PEHA−PAANa** is almost identical with that observed.

References and Notes

(1) Tuzar, Z.; Webber, S. E.; Ramireddy, C.; Munk, P. *Polym. Prepr. (Am. Chem. Soc., Div. Polym. Chem.)* **1991**, *32* (1), 525.
(2) Hurter, P. N.; Hatton, T. A.; *Langmuir* **1992,** *8*, 1291.
(3) Kiserow, D.; Procházka, K.; Ramireddy, C.; Tuzar, Z.; Munk, P.; Webber, S. E.; *Macromolecules* **1992**, *25*, 4613.
(4) Zhang, L.; Eisenberg, A.; *Science* **1995**, *268*, 1728.
(5) Chu, B.; *Langmuir* **1995**, *11*, 414.
(6) Moffit, M.; Zhang, L.; Khougaz, K.; Eisenberg, A. In *Solvents and Selforganization of Polymers*, Webber, S. E., Munk, P., Tuzar, Z., Eds., Kluver Academic Publishers: Dordrecht, The Netherlands, 1996; p 53.
(7) Almgren, M.; Brown, W.; Huidt, S.; *Colloid. Polym. Sci.* **1995**, *273*, 2.
(8) Kříž, J.; Masař, B.; Pospíšil, H.; Pleštil, J.; Tuzar, Z.; Kiselev, M. A.; *Macromolecules* **1996**, *29*, 7853.
(9) Kříž, J.; Masař, B.; Dybal, J.; Doskočilová, D. *Macromolecules* **1997**, *30*, 3302.
(10) Kříž, J.; Masař, B.; Doskočilová, D. *Macromolecules* **1997**, *30*, 4391.
(11) Kříž, J.; Masař, B.; Pleštil, J.; Tuzar, Z.; Pospíšil, H.; Doskočilová, D. *Macromolecules* **1998**, *31*, 41.
(12) Vlček, P.; Otoupalová, J.; Sikora, A.; Kříž, J. *Macromolecules* **1995**, *28*, 7262.
(13) Mrkvičková, L.; Daňhelka, J. *J. Appl. Polym. Sci.* **1990**, *41*, 1929.
(14) Ostanevich, Yu. M. *Makromol. Chem., Macromol. Symp.* **1988**, *15*, 91.
(15) Pleštil, J.; Ostanevich, Yu. M.; Bezzabotnov, V. Yu.; Hlavatá, D. *Polymer* **1986**, *27*, 1241.
(16) Tuzar, Z.; Pospíšil, H.; Pleštil, J.; Lowe, A. B.; Baines, F. L.; Billingham, N. C.; Armes, S. P. *Macromolecules* **1997**, *30*, 2509.
(17) Kratky, O. In *Progress in Biophysics*, Pergamon Press: New York, 1963; Vol. 13, p 105.
(18) Lindman, R.; Olsson, U.; Söderman, O. In *Dynamics of Solutions and Fluid Mixtures by NMR*; Delpuech, J.-J., Ed.; John Wiley: New York, 1995; p 345.
(19) Brereton M. G. *Macromolecules* **1989**, *22*, 3667.
(20) Brereton M. G. *Macromolecules* **1990**, *23*, 1119.
(21) Limpouchová, Z.; Procházka, K. *Collect. Czech. Chem. Commun.* **1993**, *58*, 2290.
(22) Procházka, K. *J. Phys. Chem.* **1995**, *99*, 14108.
(23) Schneider, B.; Pivcová, H.; Doskočilová, D. *Macromolecules* **1972**, *5*, 120.
(24) Doskočilová, D.; Schneider, B. *Adv. Colloid Interface Sci.* **1978**, *9*, 63.
(25) Doskočilová, D.; Schneider, B. *Pure Appl. Chem.* **1982**, *54*, 575.
(26) Jakeš, J. *Collect. Czech. Chem. Commun.* **1983**, *48*, 2028.
(27) Reference deleted in proof.
(28) Doskočilová, D.; Tao, D. D.; Schneider, B. *Czech. J. Phys.* **1975**, *B25*, 202.
(29) Stratton, J. A. *Electromagnetic Theory*; McGraw-Hill: New York, 1941.
(30) *CRC Handbook of Chemistry and Physics*, 73rd ed.; Lide, D. R., Ed.; CRC Press: Boca Raton, FL, 1993.
(31) Lipari, G.; Szabo, A. *J. Am. Chem. Soc.* **1982**, *104*, 4546.
(32) Lipari, G.; Szabo, A. *J. Am. Chem. Soc.* **1982**, *104*, 4559.
(33) Abragam, A. *The Principles of Nuclear Magnetism*; Clarendon Press: Oxford, England, 1961.
(34) Simon, G.; Baumann, K.; Gronski, W. *Macromolecules* **1992**, *25*, 3624.
(35) Kay, L. E.; Prestergard, J. H. *J. Am. Chem. Soc.* **1987**, *109*, 3829.
(36) Wong, T. C.; Wang, P.-L.; Duh, D.-M.; Hwang, L.-P. *J. Phys. Chem.* **1989**, *93*, 1295.

MA9809334